Mechanism-Based Inactivation of Human Cytochrome P450 1A2 by Furafylline: Detection of a 1:1 Adduct to Protein and Evidence for the Formation of a Novel Imidazomethide Intermediate†

Jagdish K. Racha, Allan E. Rettie, and Kent L. Kunze*

Department of Medicinal Chemistry, University of Washington, Seattle, Washington 98195

Received December 8, 1997; Revised Manuscript Received February 25, 1998

ABSTRACT: The rapid loss of human CYP1A2 (cytochrome P450 1A2) activity caused by the 8-methylxanthine furafylline is investigated with the aim of determining whether a stable covalent adduct of the xanthine to the enzyme could be identified. Metabolic studies employing expressed CYP1A2 with radiolabeled furafylline and a close analogue, cyclohexylline, where the furan ring is replaced with cyclohexane, indicate that these xanthines are bound in a 1:1 ratio to CYP1A2 protein. This result, combined with earlier kinetic studies, verifies that these compounds are mechanism-based inhibitors of the enzyme. The 8′-methyl carbinols are the only metabolites formed by CYP1A2, and substantial (70−80%) incorporation of oxygen from the medium into the carbinols is observed. Carbinol formation is further characterized by high intramolecular isotope effects ($k_H/k_D > 9$) and low intermolecular isotope effects ($^DV/K < 2$). Overall partition ratios are low (5.0 and 7.6, respectively), confirming our previous conclusion that furafylline is an efficient inactivator. By contrast, the N^7-methyl-8-methylxanthines are good substrates for CYP1A2 but are not themselves inactivating agents. In addition to other metabolic products, the 8′-methyl carbinols of these N^7-methyl-8-methylxanthines are formed in substantial amounts with equally high intramolecular isotope effects; however, the carbinol oxygen is derived exclusively from molecular oxygen. We conclude that oxidation of the 8-methyl group of furafylline and cyclohexylline, but not their N^7-methyl analogues, by CYP1A2 promotes a major fraction of the inactivating xanthines to a two electron oxidized intermediate which either terminates enzyme activity by reaction with an active site amino acid or is decomposed by reaction with the medium to give carbinol.

The majority of P450-catalyzed oxidation reactions proceed uneventfully to product with no deleterious effects to the enzyme or its environment. Occasionally, a portion of the reaction products are highly reactive and form adducts with a variety of intracellular targets that are critical to proper cellular function and homeostasis. More rarely, oxidative flux to products includes species which terminate enzyme activity by covalent modification of P450 protein or prosthetic heme. The study of the molecular events associated with enzyme inactivation caused by suicide substrates has provided a wealth of mechanistic and structural information relevant to P450 biochemistry (*1*). In addition, the now well-recognized propensity of certain types of functional groups to provoke catalysis-dependent enzyme inactivation has been employed to design specific irreversible inhibitors of selected P450 enzymes for use in therapeutics and as tools in drug metabolism research. Finally, suicide substrates can be highly useful probes of enzyme active site architecture, provided that the site of adduction can be determined. For instance, the pattern of covalent attachment to heme has provided unique information about the orientation of the prosthetic group. Identification of protein adducts holds even more promise, particularly if the adduct can be demonstrated to reside in the active site or the substrate access channel (*2*).

CYP1A2 is a major constitutive enzyme present in human liver that has been identified as a key factor in the bioactivation of a large number of environmental contaminants including aflatoxin, arylamines, and dietary heterocyclic amines (*3*). The 8-methylxanthine furafylline (Chart 1) is a potent inhibitor of human CYP1A2 which, by virtue of its selective effect, has found widespread use as a probe for CYP1A2-dependent activity (*4*−*9*). Clinical studies indicate that furafylline may completely suppress human CYP1A2 oxidative activity in vivo (*10*, *11*). We have shown that furafylline causes a rapid, irreversible loss of CYP1A2 activity in human liver microsomes ($K_I = 23\ \mu M$, $k_{inact} = 0.87\ min^{-1}$) (*5*). A modest intermolecular isotope effect ($k_H/k_D = 2.02$) on the rate of inactivation is observed when the 8-methyl group hydrogens are replaced by deuterium, suggesting that cleavage of an 8-methyl carbon−hydrogen bond is involved in the inactivation process.

† This work was supported by NIH Grant GM 48750 (K.L.K.) and in part by Grant GM 49054 (A.E.R.).

* To whom correspondence should be addressed: Box 357610. Telephone: 206-685-3543. E-mail: kkunze@u.washington.edu.

[1] Abbreviations: CYP1A2, human cytochrome P450 1A2; EIGC−MS, gas chromatography with electron impact mass spectrometric detection; ESLC−MS, liquid chromatography with electrospray ionization mass spectrometric detection; LC−RD, liquid chromatography with radiometric detection; TFA, trifluoroacetic acid; SDS−PAGE, sodium dodecyl sulfate−polyacrylamide gel electrophoresis; SIM, selected ion monitoring.

S0006-2960(97)03011-0 CCC: $15.00
Published on Web 04/28/1998

Chart 1

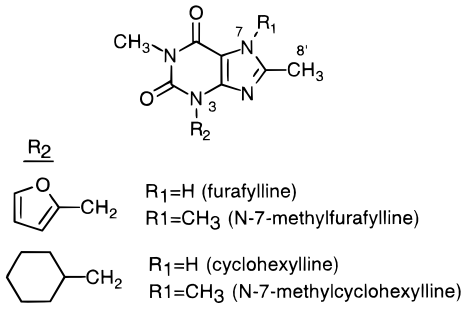

While these results are consistent with efficient irreversible modification of this enzyme by covalent attachment of a reactive intermediate to the enzyme, definitive evidence for this conclusion has not been forthcoming. One purpose of the studies reported here was to determine whether radiolabeled furafylline becomes bound to CYP1A2 with the aim of providing a rational basis for the inactivation observed. Due to concerns about the potential for bioactivation of the furan ring, parallel studies with cyclohexylline (Chart 1) were conducted. One- to-one covalent binding of furafylline and cyclohexylline equivalents to cDNA-expressed CYP1A2 protein is reported here. A second aim was to inventory the balance of metabolic products to develop information concerning the nature of the reactive intermediate which covalently modifies the enzyme. To this end, the metabolic fate of furafylline, cyclohexylline, and their N^7-methyl analogues (Chart 1) has been determined. The combined results of inactivation, covalent binding, isotope effect, and oxygen tracing studies have been utilized to expose a novel two electron oxidized electrophilic intermediate as the likely proximate inactivating species. Formation of this intermediate is suppressed when the imidazole hydrogen is replaced with a methyl group.

MATERIALS AND METHODS

Materials. [1-^{14}C]Acetic anhydride was purchased from American Radiolabeled Chemicals, Inc. (St. Louis, MO). $H_2{}^{18}O$ (95−98%) and $^{18}O_2$ (95−98%) were purchased from Cambridge Isotope Laboratories (Andover, MA). All other chemicals were purchased from Aldrich Chemical Co. (Milwaukee, WI) or Sigma (St. Louis, MO). Liquid scintillation cocktails EcoLume, CytoScint ES (ICN Biomedicals, Inc. (Irvine, CA)), and Flo-Scint II (Packard Instrument Company (Meriden, CT)) were used for quantitation of ^{14}C. Microsomes prepared from lymphoblastoid cells containing cDNA-expressed human cytochrome CYP1A2 (M103b) were purchased from Gentest (Woburn, MA). Human liver microsomes were prepared as described (*5*).

Instruments. ^{1}H NMR spectra were recorded on a Varian 300 or a Bruker AM500 instrument. Hewlett-Packard 1100 or 1050 systems were used for routine HPLC analysis with UV detection at 280 nm. A Radiomatic Flo-one-β model 150TR detector (Packard Instruments Company, Meriden, CT) using Flo-Scint-II was employed for quantitation of HPLC eluents. A Packard Tricarb 2200CA (Packard Instruments Company, Downers Grove, IL) was used for other radioassays. Melting points (uncorrected) were determined on a capillary melting point apparatus (Arthur H. Thomas Company, Philadelphia, PA).

Gas Chromatography−Mass Spectrometry. EIGC−MS analysis was performed on a Micromass Trio 2000 quadrupole mass spectrometer (Micromass Ltd., Cheshire, U.K.) coupled to a Hewlett-Packard 5890 gas chromatograph and a Hewlett-Packard 7673A autosampler (Hewlett-Packard, Palo Alto, CA). A J&W (Folsom, CA) DB-5 (30 m × 0.32 mm i.d., 25-μm film thickness) capillary column was used for all analyses. Helium was used as the carrier gas at a head pressure of 5 psi. Injector, interface, and detector temperatures were set at 250, 200, and 250 °C, respectively. Samples were injected at a column temperature of 120 °C, which was held for 1 min, followed by a linear 12 °C/min ramp to 300 °C, which was held for 4 min. Retention times for N^7-methylfurafylline, N^7-methylcyclohexylline, N^7-methyl-8′-O-TMS-furafylline, N^7-methyl-8′-O-TMS-cyclohexylline, N^7-methyl-O-TMS metabolite 1 of cyclohexylline, and N^7-methyl-O-TMS metabolite 2 of cyclohexylline analytes were 12.59, 12.99, 13.61, 13.92, 14.67, and 15.24 min, respectively. Integrated ion currents generated at an electron energy of 11 eV monitored in the SIM mode (0.15-ms dwell) were used for isotope effect studies.

Liquid Chromatography−Mass Spectrometry. ESLC−MS analyses were carried out on a Micromass Quattro II tandem quadrupole mass spectrometer (Micromass Ltd., Manchester, U.K.) coupled to an HPLC (Shimadzu LC-10AD with SPD-10AV UV−vis variable detector (Shimadzu Scientific Instruments, Inc., Columbia, MD)). Isocratic separation of analytes was achieved on Waters μBondapak C_{18} 3.9 × 300 mm, 5 μm HPLC column. The source temperature was 100 °C with the cone voltage set to 30 V. Solvent flow through the column was 1 mL/min with 10% of the flow being diverted to the mass spectrometer. For the substrates furafylline and N^7-methylfurafylline the mobile phase consisted of acetonitrile:methanol:water (5:30:65). 8′-OH-Furafylline, N^7-methyl-8′-OH-furafylline, furafylline, and N^7-methylfurafylline eluted at 5.5, 7.1, 9.2, and 13.5 min, respectively. The mobile phase composition for substrates cyclohexylline and N^7-methylcyclohexylline was acetonitrile:methanol:water (20:20:60). Metabolite 1 of N^7-methylcyclohexylline, metabolite 2 of N^7-methylcyclohexylline, 8′-OH-cyclohexylline, N^7-methyl-8′-OH-cyclohexylline, cyclohexylline, and N^7-methylcyclohexylline eluted at 2.8, 3.4, 10.7, 14.9, 19.1 and 25.9 min, respectively. Scan data were collected over a range of 50−450 Da. SIM studies were carried out on the protonated parent ion cluster (four successive masses). Integrated peak area ratios were used for all calculations.

Synthesis. The synthesis of furafylline, 8′-[$^2H_1$]furafylline, and 8′-OH-furafylline from 1-(furfuryl)-3-methyl-5,6-diaminouracil have been previously described (*5*). The ESMS spectra of furafylline [*m*/*z* 261 $[M + H]^+$ (100%), 193 $[M - C_4H_3O]^+$ (10%), 81 $[C_5H_5O]^+$ (41%)] and 8′-OH-furafylline [*m*/*z* 277 $[M + H]^+$ (100%), 259 $[M - OH]^+$ (8%), 209 $[M - C_4H_3O]^+$ (9%), 81 $[C_5H_5O]^+$ (29%)] are reported here.

1-(Cyclohexylmethyl)-3-methyl-5,6-diaminouracil. This precursor was prepared in an identical fashion in an overall yield of 60% based on methylisocyanate and cyclohexanemethylamine (26.2 g): mp (aqueous ethanol, 1:1) 194−97 °C; ^{1}H NMR (300 MHz, Me_2SO-d_6) δ 6.14 (s, 2H), 3.73 (d, J = 7.4 Hz, 2H), 3.13 (s, 3H), 2.93 (s, 2H), 1.52−1.59 (m, 6H), 1.08−1.12 (m, 5H).

Cyclohexylline [3,7-Dihydro-1,8-dimethyl-3-(cyclohexylmethyl)-1H-purine-2,6-dione]. The 5,6-diaminouracil (5.04 g, 0.02 mol) was heated at reflux under argon in a solution of 25 mL of acetic anhydride for 2 h. The solvent was removed in vacuo, and the residue was dissolved in 10% aqueous NaOH and heated to reflux for 2 h. The cooled solution was acidified with concentrated HCl to pH 4, and the precipitate was collected, filtered, dissolved in a minimum volume of hot ethanol, decolorized with activated charcoal (0.5 g), and filtered through a bed of diatomaceous earth. The solid remaining after solvent removal from the filtrate was crystallized from ethanol:water (1:1) to give 4.3 g (78%) of cyclohexylline: mp 248−49 °C; ^{1}H NMR (300 MHz, $CDCl_3$) δ 3.99 (d, J = 7.4 Hz, 2H, N_3-CH_2), 3.48 (s, 3H, N_1-CH_3), 2.61 (s, 3H, C_8-CH_3), 1.99 (br, 1H), 1.63−1.74 (m, 6H), 1.13−1.25 (m, 4H); ESMS *m*/*z* 277 $[M + H]^+$ (100%), 181 $[M - C_7H_{13}]^+$ (9%).

8′-[$^2H_3$]-Cyclohexylline [3,7-Dihydro-1-methyl-8-[$^2H_3$]-methyl)-3-(cyclohexylmethyl)-1H-purine-2,6-dione]. The diaminouracil (0.63 g) was heated to reflux under an argon atmosphere with 3 mL of D_6-acetic anhydride (99 atom % D) for 4 h. The solvent was removed in vacuo, and the residue was dissolved in 10% NaOD/D_2O and heated to reflux for 2 h. The cooled solution was acidified with concentrated HCl to pH 4, and the precipitate was collected, filtered, dissolved in a minimum volume of hot ethanol, decolorized with activated charcoal (60 mg), and twice crystallized from ethanol:water (1:1) to give D_3-cyclohexylline (0.52 g, 74%): mp (aqueous ethanol, 1:1) 247−48 °C; ^{1}H NMR (300 MHz, $CDCl_3$) δ 3.99 (d, J = 7.4 Hz, 2H, N_3-CH_2), 3.47 (s, 3H, N_1-CH_3), 1.95−1.99 (br, 1H), 1.53−1.77 (m, 6H), 1.11−1.25 (m, 4H).

[8-^{14}C]Furafylline and [8-^{14}C]-Cyclohexylline. 1-(Furylmethyl)-3-methyl-5,6-diaminouracil (0.11 mmol) was heated at reflux under argon in a solution of 1.0 mCi of [1-^{14}C]-acetic anhydride (0.1 mmol, 10 mCi mmol^{-1}) and 0.5 mL dry pyridine for 2 h. The reaction mixture was cooled, and 2 mL of 10% aqueous NaOH was added and heated to reflux for 1 h. The cooled solution was acidified with concentrated HCl to pH 5−6, and the product was extracted (2×) with 5 mL of ethyl acetate. The product [8′-^{14}C]furafylline was purified by HPLC on a Whatman Partisil 5 ODS-3 column. Yield: 14.3 mg (50%, sp act. 5 mCi mmol^{-1}). [8′-^{14}C]-Cyclohexylline was synthesized in a similar manner with [1-^{14}C]acetic anhydride (0.1 mmol, 55 mCi mmol^{-1}). Yield: 14.9 mg (54%, sp act. 27.5 mCi mmol^{-1}).

8′-OH-cyclohexylline [3,7-Dihydro-1-methyl-8-(hydroxymethyl)-3-(cyclohexylmethyl)-1H-purine-2,6-dione]. 1-(Cyclohexylmethyl)-3-methyl-5,6-diaminouracil (2.52 g, 0.01 mol) was refluxed with 10 mL of ethyl glycolate for 4 h in an argon atmosphere. The reaction was worked up as described above, and the product was crystallized from ethanol:water (1:1) to give 2.42 g (83%) of 8′-OH-cyclohexylline: mp 242−43 °C; ^{1}H NMR (300 MHz, $CDCl_3$ + Me_2SO-d_6) δ 4.79 (s, 2H, C_8-CH_2), 3.97 (d, J = 7.4 Hz, 2H, N_3-CH_2), 3.40 (s, 3H, N_1-CH_3), 1.92−1.96 (br, 1H), 1.60−1.69 (m, 6H), 1.09−1.25 (m, 4H); ESMS *m*/*z* 293 $[M + H]^+$ (100%), 275 $[M - OH]^+$ (22%), 197 $[M-C_7H_{13}]^+$ (5%).

8′-[$^2H_1$]Furafylline and 8′-[$^2H_1$]Cyclohexylline. The 8′-carbinols above (50 mg) were treated with equimolar amounts of methanesulfonyl chloride in dry pyridine for 36 h at 20−25 °C under an N_2 atmosphere. Attempts to isolate the mesylates were unsuccessful, so instead, the pyridine was evaporated by warming under a stream of dry N_2 and the residue was treated with a 4-fold excess of $LiAlD_4$ in anhydrous THF by stirring overnight under an N_2 atmosphere. Excess $LiAlD_4$ was destroyed by addition of ice-cold H_2O followed by the addition of aqueous NaOH. The reaction mixture was filtered, and the filtrate was adjusted to pH 6 with diluted HCl. The product was extracted with ethyl acetate and purified on a Partisil 5 ODS-3 preparative column by HPLC. Deuterium contents in the 8-methyl groups of furafylline and cyclohexylline were determined by EIGC−MS analysis of the parent ion envelopes of the N^7-methyl derivatives (see below for preparation) at an electron energy of 11 eV. Fractional deuterium contents [d_1/(d_1 + d_0)] in the 8-methyl groups of N^7-methylfurafylline and N^7-methylcyclohexylline were 97.83 ± 0.03% and 98.56 ± 0.04%, respectively.

N^7-Methylxanthines and N^7-Methylxanthine 8′-Carbinols. The general procedure for unlabeled and labeled xanthines is as follows. A mixture of the xanthine (0.001 mol), methyl iodide (0.31 mL, 0.005 mol), and K_2CO_3 (0.69 g, 0.005 mol) in acetone (10 mL) was stirred overnight at 40 °C. The products were crystallized following filtration and solvent removal (yields >90%). N-Alkylation of 1,3-dialkylxanthines occurs with a high preference for the N^7 position (*12*). ^{1}H NMR (500 MHz) nuclear Overhauser effect (NOE) studies of the furan analogues below in degassed $CDCl_3$ confirmed the assignments. As expected, reciprocal enhancements (ca. 10%) were observed between N^7-methyl or methylene and 8-methyl or 8-hydroxymethyl methylene protons. No enhancement of the N^3 methylene protons was observed upon irradiation of the N^7-methyl or methylene protons and vice versa.

N^7-Methylfurafylline: mp (aqueous ethanol 1:1) 182−84 °C; ^{1}H NMR (300 MHz, $CDCl_3$) δ 7.33 (d, J = 2.0 Hz, 1H, $C_{5'}-H$), 6.54 (d, J = 3.3 Hz, 1H, $C_{3'}-H$), 6.30 (dd, J = 2.0 and 3.3 Hz, 1H, $C_{4'}-H$), 5.32 (s, 2H, N_3-CH_2), 3.92 (s, 3H, N_7-CH_3), 3.39 (s, 3H, N_1-CH_3), 2.56 (s, 3H, C_8-CH_3); ESMS *m*/*z* 275 $[M + H]^+$ (100%), 207 $[M - C_4H_3O]^+$ (35%), 81$[C_5H_5O]^+$ (20%).

N^7-Methyl-8′-OH-furafylline: mp (acetone) 150−52 °C; ^{1}H NMR (300 MHz, $CDCl_3$) δ 7.35 (d, J = 1.8 Hz, 1H, $C_{5'}-H$), 6.52 (d, J = 3.0 Hz, 1H, $C_{3'}-H$), 6.32 (dd, J = 1.8 and 3.0 Hz, 1H, $C_{4'}-H$), 5.31 (s, 2H, N_3-CH_2), 4.88 (s, 2H, C_8-CH_2), 4.19 (s, 3H, N_7-CH_3), 3.41 (s, 3H, N_1-CH_3); ESMS *m*/*z* 291 $[M + H]^+$ (100%), 223 $[M - C_4H_3O]^+$ (22%), 81 $[C_5H_5O]^+$ (29%).

N^7-Methylcyclohexylline: mp (aqueous ethanol, 1:1) 178−79 °C; ^{1}H NMR (300 MHz, $CDCl_3$) δ 3.96 (d, J = 7.6 Hz, 2H, $N-CH_2$), 3.94 (s, 3H, N_7-CH_3), 3.41 (s, 3H, N_1-CH_3), 2.52 (s, 3H, C_8-CH_3), 1.93−1.97 (br, 1H); 1.63−1.73 (m, 6H), 1.11−1.20 (s, 4H); ESMS *m*/*z* 291 $[M + H]^+$ (100%), 195 $[M - C_7H_{13}]^+$ (4%).

N^7-Methyl-8′-OH-cyclohexylline: mp (acetone) 143−45 °C; ^{1}H NMR (300 MHz, $CDCl_3$) δ 4.96 (s, 2H, C_8-CH_2), 4.12 (s, 3H, N_7-CH_3), 4.03 (d, J = 7.6 Hz, 2H, N_3-CH_2). 3.43 (s, 3H, N_1-CH_3), 1.92−1.98 (br, 1H), 1.63−1.76 (m, 6H), 1.16−1.24 (m, 4H); ESMS *m*/*z* 307 $[M + H]^+$ (100%), *m*/*z* 289 $[(M + H)^+ - H_2O]$ (11%), 211 $[M - C_7H_{13}]^+$ (4%).

N^7-n-Propylfurafylline. This compound was prepared as above with substitution of *n*-propyl iodide for methyl iodide: mp 123−125 °C; ^{1}H NMR (300 MHz, $CDCl_3$) δ 7.34 (d, J = 2.0 Hz, 1H, $C_{5'}$−H), 6.48 (d, J = 3.3 Hz, 1H, $C_{3'}$−H), 6.31 (dd, J = 2.0 Hz & 3.3 Hz, 1H, $C_{4'}$−H), 5.28 (s, 2H, N_3−CH_2), 4.21 (t, J = 7.3 Hz, 2H, N_7−CH_2), 3.39 (s, 3H, N_1−CH_3), 2.52 (s, 3H, C_8−CH_3), 1.83 (m, 2H, N_7−2′-CH_2), 0.97 (t, 3H, N_7−3′-CH_3); EIMS (70 eV) *m*/*z* 274 $[M]^+$ (62%), 81 $[C_5H_5O]^+$ (100%).

Time-Dependent Loss of Human Liver CYP1A2 Activity. Each xanthine (90 μM) was preincubated with human liver microsomes, HLM110, for 3 min at 37 °C followed by the addition of buffer or NADPH (1 mM final concentration) (*5*). The final concentration of total P450 in these incubations was 3 μM. At selected time intervals (0, 1.5, 3.0, 5.0, and 15 min), 50-μL aliquots of the incubation mixtures were transferred to tubes containing 950 μL of (*R*)-warfarin (3 mM) and NADPH in buffer and incubated for 20 min (activity assay). The reactions were quenched with 0.6 mL of acetone and assayed for (*R*)-6-hydroxywarfarin by selected ion EIGC−MS (*5*). Rates of formation of 6-hydroxywarfarin at time 0 min were taken as 100% activity to allow for the time required for mixing and to transfer this aliquot to the activity assay (10 s).

Metabolic Studies with Lymphoblastoid CYP1A2 Microsomes. Radiolabeled or unlabeled xanthines (30 μM) were preincubated with CYP1A2 for 3 min at 37 °C followed by the addition of NADPH (final concentration, 1.0 mM) or buffer. The final concentration of CYP1A2 in these incubation mixtures (0.6 mL) was 0.213 μM (2 mg of protein). The incubations were terminated at 30 min by addition of 0.1 mL of cold 50% aqueous trifluoroacetic acid (TFA). The samples were vortexed and then centrifuged at 3000 rpm for 10 min using a Beckman GS-6R centrifuge at 0−5 °C. The supernatants were analyzed for metabolites by LC−RD for ^{14}C substrates or ESLC−MS in the scan mode for nonradiolabeled substrates (see general conditions below). Retention times and fragmentation patterns were compared with authentic metabolite standards when available.

Time-Dependent Formation of 8′-OH-Furafylline and Irreversibly Bound Protein Equivalents. [8-^{14}C]Furafylline (30 μM) was preincubated with HLM110 microsomes for 3 min at 37 °C followed by the addition of NADPH. The total incubation volume was 15 mL. The final concentrations of NADPH and total P450 were 1 mM and 5.15 μM, respectively. At selected time intervals (0, 1, 3, 5, 7, 10, 15, 20, and 30 min), triplicate 0.5-mL aliquots were transferred to tubes containing 0.2 mL of 30% cold aqueous TFA. After centrifugation, aliquots of the separated supernatants were analyzed for 8′-OH-furafylline by HPLC−RD. The pellet was resuspended in 7 mL of cold sulfuric acid:methanol (5%, v/v), vortexed, and centrifuged, and the supernatant was removed for scintillation counting. This cycle was repeated six times until background counts in the supernatants were achieved. The final pellet was dissolved in 1.5 mL of 1.0 M aqueous NaOH at 60 °C for 1 h. Aliquots (0.5 mL) were added to 1 mL of water and 10 mL of EcoLume, vortexed for 30 s, and stored overnight in the counter before determination of bound radioactivity.

Effect of Trapping Agents on Carbinol Formation and Protein Binding. Radiolabeled xanthines (60 μM) were preincubated with 0.4 μM CYP1A2 in an incubation volume of 0.6 mL for 3 min at 37 °C. Final concentrations of the trapping agents added in buffer were sodium cyanide (1 mM), *N*-acetylcysteine (8 mM), or glutathione (2 mM). Control incubations were carried out with enzyme and substrate with and without addition of NADPH. Radioactive equivalents (8′-OH-xanthine or protein adduct) were determined as above. Similar incubations were carried out with the N^7-methylxanthines (60 μM) for analysis of NADPH dependent protein binding in the absence of trapping agents only.

SDS−PAGE Studies. Duplicate incubations (0.667 mL) of furafylline or cyclohexylline (30 μM) with cDNA-expressed CYP1A2 (0.49 μM) were analyzed for metabolites, general protein binding, and binding to proteins resolved by SDS−PAGE. Spectral CYP1A2 content was determined as described previously (*5*). Incubations were carried out for 30 min in the presence or absence of NADPH (1 mM). At this time aliquots (0.120 mL) of the incubation mixture were transferred to tubes containing 0.375 mL of gel loading buffer, immersed in boiling water for 2 min, and centrifuged for 2 min at 3000 rpm. Cold aqueous TFA (0.12 mL) was added to the balance of the incubation mixture (0.547 mL), and amounts of carbinol and bound equivalents were determined as above. An aliquot of each final pellet after dissolution in 1.0 M NaOH was removed and analyzed for protein content (BCA assay). Aliquots (0.103 mL) of the SDS-solubilized proteins were loaded onto 9% polyacrylamide gels of 1.5 mm thickness. Purified CYP2C9 and CYP2C19 were included as markers in adjacent lanes. After electrophoresis and staining, each lane of the gel was cut into 25 4-mm slices. The grid of gel slices was arranged such that the region between CYP2C9 (apparent molecular mass (SDS−PAGE) = 55 kDa) and CYP2C19 (apparent molecular mass (SDS−PAGE) = 50 kDa) was taken in a single slice. At the time these studies were conducted, purified CYP1A2 was not available to us. Each gel slice was placed in a scintillation vial and dissolved in 1 mL of 85% hyamine hydroxide at 60−65 °C. After 12 h, the vials were cooled and 10 mL of CytoScint ES was added to the sample, which was then shaken vigorously and allowed to sit overnight in the counter before counting. Similar studies were carried out for the *N*-methylxanthines.

Isotope Effect Studies. The xanthine carbinol metabolites could be efficiently extracted from incubation mixtures; however, efforts to analyze 8′-OH-xanthine carbinols as well as the parent xanthines by capillary GC−MS using a DB-5 column without prior derivatization were unsuccessful. Good chromatographic results for synthetic standards of substrate and metabolites could be achieved when active hydrogens (imidazole N−H and carbinol O−H) were replaced with a methyl (methyl iodide) and a trimethylsilyl group (BSTFA), respectively. The N^7-methyl-8′-O-TMS carbinol derivatives were readily identified in organic extracts of NADPH-fortified incubation mixtures by EIGC−MS analysis based on the comparison of fragmentation patterns and retention times with authentic standards.

[8′-$^2H_1$]Xanthines or a 1:1 mixture of [8′-$^2H_3$]- and [8′-$^1H_3$] xanthines (60 μM) were incubated with CYP1A2 (0.1 μM) for 30 min in the presence of NADPH (1 mM). The reaction mixtures were extracted with two portions of ethyl acetate (5 mL), and the combined organic layers were dried over anhydrous $MgSO_4$. For furafylline and cyclohexylline incubations the residues, after solvent removal, were treated

with methyl iodide as above to methylate the N^7-nitrogen. The solutions were then filtered, and solvent was removed by evaporation under a stream of nitrogen. The residues were treated with 50 uL of 20% (v/v) BSTFA in acetonitrile at room temperature for 12 h. For N^7-methylxanthine incubations the residues were treated with BSTFA only. To determine intermolecular isotope effects on N^7-demethylation of N^7-methylfurafylline, the incubation extracts were first treated with propyl iodide in acetone in the presence of potassium carbonate to generate the analyte N^7-propylfurafylline.

Deuterium contents in the derivatized carbinols and substrates (separate runs) were determined by EIGC−MS (electron energy, 11 eV) of the appropriate parent ion isotope manifolds (M − 1 to M + 3) in the SIM mode. Integrated peak area ratios were corrected for natural abundances determined from separate runs with authentic standards to obtain estimates of deuterium content in the carbinol products and substrates. By this method, ion fractions M − 1/(M + M − 1) for the N^7-methylated protio substrates furafylline and cyclohexylline were 0.19% and 0.22%, while the corresponding M − 1 fractions for the N^7-methyl-8′-O-TMS carbinol derivatives were 0.36% and 0.33%, respectively. Fractional deuterium contents $d_2/(d_2 + d_0)$ or $d_1/(d_1 + d_0)$] in the carbinols were determined in triplicate. Intermolecular isotope effects were calculated by standard methods (*13*). Intramolecular isotope effects were calculated as $k_H/k_D = 0.5fd_1/(fd_0 - fSd_0)$ where fd_1 and fd_0 are the mole fractions of monodeutero and protio carbinols, respectively, and fSd_0 is the mole fraction of protio substrate in the d_1 substrate (*14*). Calculations were made with full propagation of errors.

$H_2{}^{18}O$ Incorporation Experiments. Incorporation of oxygen from the medium into the xanthine metabolites was assessed by ESLC−MS analysis of incubations of CYP1A2 with each of the four xanthines in the presence of $H_2{}^{18}O$ (47.5%) and NADPH (1 mM). These incubations were carried out at a substrate concentration of 60 μM with 0.1 μM CYP1A2 in 80 mM potassium phosphate buffer (pH 7.4). The metabolites were extracted with ethyl acetate as above, and the residue after solvent evaporation was reconstituted in 0.1 mL of methanol for ESLC−MS analysis. The protonated parent ion envelopes were monitored in the selected ion mode, and integrated peak areas were used for quantitation. Corrections were made by measurement of authentic metabolite ion ratios or by measurement of the ratios from incubations conducted under standard conditions when authentic metabolite was unavailable. Fractional $H_2{}^{18}O$ content in the lot used in these studies (95%) was determined by introduction of an aliquot into the sample inlet port of a VG 70/70 mass spectrometer operating in the electron impact mode (electron energy, 70 eV) and measurement of the ratio of 20 Da to 18 Da ion currents. The 8-methyl carbinols of furafylline and cyclohexylline formed in the presence of $H_2{}^{18}O$ were analyzed for ^{18}O content by EIGC−MS as well, following a protocol similar to that for the isotope effect studies. The mole fraction of ^{18}O in the carbinol was divided by the mole fraction of ^{18}O in the medium to obtain corrected levels of incorporation of ^{18}O into the carbinols.

$^{18}O_2$ Incorporation Experiments. Incorporation of ^{18}O from molecular oxygen was determined by incubating, in a pairwise manner, furafylline (5 μM) and N^7-methylcyclohexylline (30 μM) or cyclohexylline (5 μM) and N^7-methylfurafylline (30 μM) under an atmosphere of $^{18}O_2$ in screw-capped test tubes fitted with a Teflon septum. Incubations were carried out with 0.1 μM CYP1A2 in 100 mM potassium phosphate buffer (pH 7.4) in a total volume of 1.0 mL. The tubes were exposed to two vacuum evacuation purge cycles with argon on ice with gentle swirling of the incubation mixtures prior to introduction of ^{18}O oxygen into the tubes via a tube and needle, the contents of which were also exposed to the purge cycles. The reactions were initiated with 50 uL of cold argon-saturated NADPH to a final concentration of 1 mM via a gastight syringe. At the end of 30 min the incubations were terminated by introduction of 1 mL of ethyl acetate and analyzed for ^{18}O content in the 8-methyl carbinols by ESLC−MS as described above.

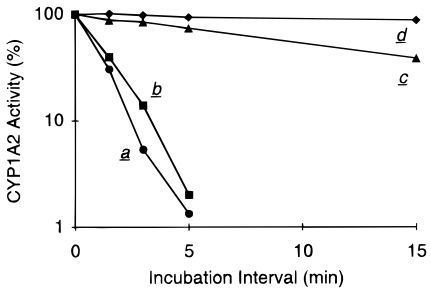

FIGURE 1: Effect of time of incubation of 8-methylxanthines and NADPH with human liver microsomes, HLM110, on CYP1A2-dependent formation of (*R*)-6-hydroxywarfarin in subsequent activity assays. Incubation times given are post addition of NADPH. P450 content in the activity assays was 5% of that in the preincubation assays. The concentration of each 8-methylxanthine, (a) cyclohexylline, (b) furafylline, (c) N^7-methylcyclohexylline, or (d) N^7-methylfurafylline was 90 μM.

RESULTS

Effect of 8-Methylxanthines on CYP1A2 Activity. Furafylline, N^7-methylfurafylline, cyclohexylline, and N^7-methylcyclohexylline were each incubated with HLM110 microsomes at a concentration of 90 μM. Time-dependent loss of CYP1A2 activity was determined as before (*5*) but in a more abbreviated manner. Rapid first-order loss of CYP1A2 activity was observed with furafylline ($k = 0.77$ min^{-1}) and cyclohexylline ($k = 0.89$ min^{-1}) (Figure 1). N^7-Methylcyclohexylline caused a more modest loss of activity ($k = 0.06$ min^{-1}). Loss of activity with N^7-methylfurafylline ($k = 0.009$ min^{-1}) was comparable to that of control (no inhibitor: $k = 0.01$ min^{-1}).

Identification and Quantitation of 8-Methylxanthine Metabolites. Radiolabeled and unlabeled xanthines were incubated with CYP1A2 microsomes at a concentration of 30 μM for 30 min in the presence or absence of NADPH. Aliquots of the supernatants, following precipitation of protein and centrifugation, were analyzed for metabolites by reversed-phase HPLC using a radiometric detector (LC−RD) (Figure 2) or ESLC−MS. No radiolabeled metabolites were observed in the absence of NADPH. Where possible, authentic metabolites were used to confirm metabolite structures on the basis of retention time and mass fragmentograms. Amounts of each product formed in the original incubation mixtures are given in the caption of Figure 2.

A single radioactive peak which co-eluted with authentic 8′-OH-furafylline was formed by the NADPH-dependent metabolism of furafylline (Figure 2A, peaks a and b,

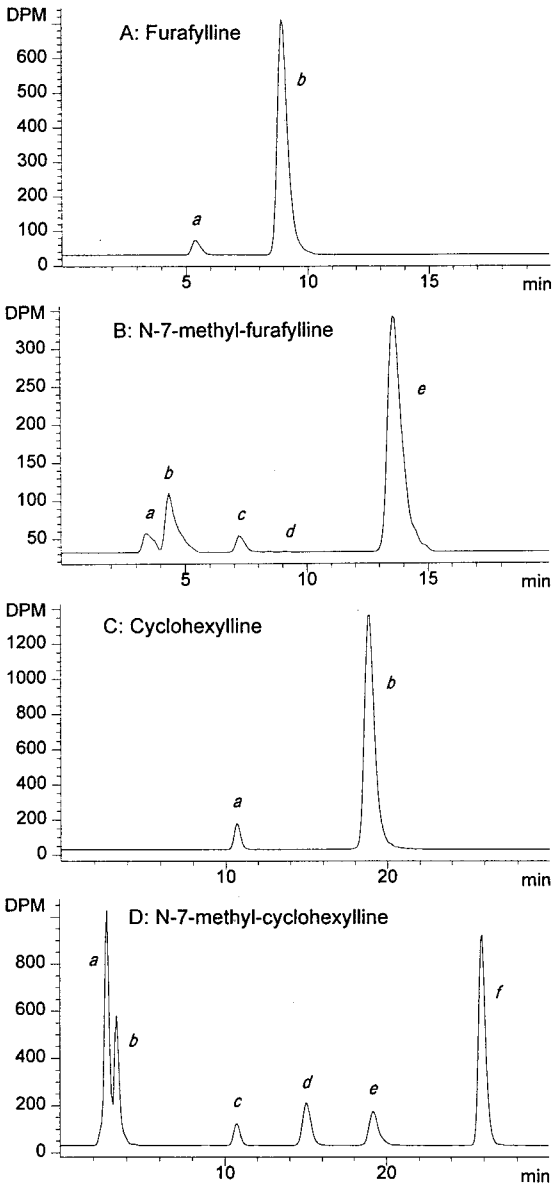

FIGURE 2: Isocratic HPLC radiochromatographic profiles of supernatants of incubations of ^{14}C-xanthines (30 μM) with cDNA-expressed CYP1A2 (128 pmol). Amounts of identified metabolites provided are corrected back to the original incubation mixtures. Solvent compositions were acetonitrile:methanol:water (5:30:65) for furafylline and N^7-methylfurafylline or acetonitrile:methanol: water (20:20:60) for cyclohexylline and N^7-methylcyclohexylline. Panel A: (a) 8′-OH-Furafylline (5.4 min, 670 pmol) and (b) furafylline (8.9 min). Panel B: (a) Unknown furan metabolite 1 (3.4 min, 480 pmol), (b) unknown furan metabolite 2 (4.3 min, 1640 pmol), (c) N^7-methyl-8′-OH-furafylline (7.2 min, 343 pmol), (d) furafylline (8.9 min, 31 pmol), and (e) N^7-methylfurafylline (13.6 min). Panel C: (a) 8′-OH-Cyclohexylline (10.7 min, 930 pmol) and (b) cyclohexylline (18.9 min). Panel D: (a) N^7-Methylcyclohexylline-(cyclohexyl alcohol 1) (2.8 min, 4770 pmol), (b) N^7-methylcyclohexylline-(cyclohexyl alcohol 2) (3.4 min, 2860 pmol), (c) 8′-OH-cyclohexylline (10.7 min, 670 pmol), (d) N^7-methyl-8′-OH-cyclohexylline (15 min, 1430 pmol), (e) cyclohexylline (19.1 min, 1360 pmol), and (f) N^7-methylcyclohexylline (25.9 min).

respectively). Comparison of ESLC−MS mass fragmentograms of this metabolite generated from nonradiolabeled substrate and authentic standard obtained on the same day confirmed this assignment. Likewise, CYP1A2 metabolism of cyclohexylline produced a single radioactive matabolite peak (Figure 2C, peak a) which was confirmed as 8′-OH-cyclohexylline by comparison with authentic material by ESLC−MS studies.

Five major peaks were observed in the radiochromatograms for N^7-methylcyclohexylline (Figure 2D). Peaks c, d, and e exhibited the same retention times and mass fragmentograms as authentic 8′-OH-cyclohexylline, N^7-methyl-8′-OH-cyclohexylline, and cyclohexylline, respectively. Mass fragmentograms of the unknown peak a metabolite (*m*/*z* 329 (11%) $[M + Na]^+$, 307 100%) $[M + H]^+$, 289 (30%) $[M - OH]^+$, 207 (22%), and 195 (20%)) and the peak b metabolite (*m*/*z* 329 (18%) $[M + Na]^+$, 307 (55%) $[M + H]^+$, 289 (100%) $[M - OH]^+$, 207 (19%), and 195 (13%)) indicated addition of one oxygen atom to the substrate. Two mass unit shifts of the parent ions (*m*/*z* 309) and the sodium adducts, but not of the fragment ions, were observed for these latter metabolites generated under an atmosphere of $^{18}O_2$. The minor fragment ion at *m*/*z* 195 for both metabolites is consistent with loss of an ^{18}O-labeled methylene cyclohexanol side chain to give the protonated 3-dealkylated xanthine cation. This fragment was also observed in the parent xanthine. These two metabolites are therefore the result of hydroxylation of the cyclohexane ring. The propensity of metabolite b to undergo dehydration with loss of O_2-derived oxygen suggests that the hydroxyl group resides on the cyclohexyl methine carbon.

Three major metabolite peaks were observed in the radiochromatograms for N^7-methylfurafylline (Figure 2B). The latest eluting peak (7.2 min) was identified as N^7-methyl-8′-OH-furafylline. No 8′-OH-furafylline was detected; however, a small amount of furafylline (1% of products) was observed (9.2 min), and its identity was confirmed by ESLC−MS analysis. The early eluting peaks appear to be products of oxidation of the furan ring. The electrospray mass spectrum of the larger of these peaks (4.3 min) displayed the following ions: *m*/*z* 345 (15%) $[M + K]^+$, 329 (55%) $[M + Na]^+$, 307 (75%) $[M + H]^+$, 289 (30%), and 195 (100%). The base peak ion at *m*/*z* 195 is the same fragment as that observed for the cyclohexyl ring hydroxylated products of N^7-methylcyclohexylline, which has been assigned to the protonated 3-dealkylated xanthine cation. This assignment appears to be correct since a 1 mass unit shift is observed for each of the ions in this metabolite when monodeuterated N^7-methylfurafylline is used as the substrate. A total mass of 32 Da has been added to the substrate, but no mass shifts were observed upon incubation with $^{18}O_2$ or $H_2{}^{18}O$, indicating that any oxygen introduced into the modified furan ring is rapidly lost by exchange with bulk water during sample workup and chromatography. Further study of the structure of these metabolites has not been pursued.

Additional radioactive metabolic products, observed as single broad peaks (retention times, 2−3 min), from cyclohexylline and furafylline were seen when human liver microsomes (HLM110) were used instead of CYP1A2 microsomes (not shown). Beyond the readily identified 8-methyl carbinols, more polar products were also observed, suggesting that other P450 enzymes might also metabolize these xanthines to the 8′-carbinols. The polar products, 130% and 200% of the carbinols, respectively, and the enzymes that produce them are currently under investigation.

Deuterium Isotope Effects. Intramolecular deuterium isotope effects for carbinol formation from the 8-methyl monodeutero substrates catalyzed by CYP1A2 were deter-

Table 1: Deuterium Isotope Effects for Formation of Xanthine 8′-Carbinols by CYP1A2[a]

substrate	intramolecular	intermolecular
furafylline	9.09 ± 0.08	1.8 ± 0.1
cyclohexylline	9.65 ± 0.24	1.7 ± 0.1
N^7-methylfurafylline	9.91 ± 0.11	9.9 ± 0.3
N^7-methylcyclohexylline	9.74 ± 0.22	2.8 ± 0.1

[a] Deuterium content in the product carbinols was determined by EIGC−MS analysis of the parent ion isotope cluster of the derivatized carbinols. Intramolecular isotope effects were calculated with correction for the fraction of substrate which did not contain deuterium.

mined by EIGC−MS. High intramolecular kinetic isotope effects ($k_H/k_D > 9$) were observed for carbinol formation from the four substrates (Table 1). Labeled and unlabeled substrate and product ion currents were carefully examined to ensure that all corrections were made appropriately, since the change in fractional deuterium content from substrate to product necessary to produce an isotope effect of this magnitude is small. While the primary isotope effects (P) cannot be determined from these data, it is reasonable to expect that normal secondary isotope effects (S) are operative, in which case the primary isotope effects ($P = S \times k_H/k_D$) for 8-methyl oxidation would be greater than the isotope effects observed (*14*).

Competitive intermolecular deuterium isotope effects ($^DV/K$) on the carbinol formation were also determined using equimolar mixtures of the 8′-$^2H_3$-labeled and unlabeled methylxanthines (Table 1). Low intermolecular isotope effects for carbinol formation were found for furafylline (1.8), cyclohexylline (1.7), and N^7-methylcyclohexylline (2.8), while N^7-methylfurafylline gave a surprisingly high isotope effect (9.9). $^DV/K$ values for an isotopically sensitive step may range from 1 to the intrinsic isotope effect (PS^2 in this experimental design (*14*)) depending on the availability of alternative pathways and the dynamics of substrate movement in the active site (*15*). When, as is the case for N^7-methylfurafylline, $^DV/K$ approaches the intrinsic isotope effect, the corresponding $^DV/K$ for a nonisotopically sensitive step (N^7-demethylation) should be 1 or inverse. In any event, a significant inverse isotope effect is diagnostic for a nondissociative mechanism, while a value of 1 is accommodated by all alternatives including a general nondissociative mechanism with the exception of a rapid equilibrium nondissociative mechanism (*15*). Accordingly, the ratio of [8′-$^2H_3$]- to [8′-H_3]furafylline formed in the intermolecular experiment with N^7-methylfurafylline was determined by EIGCMS analysis of N^7-propylfurafylline obtained by treatment of the incubation extracts with propyl iodide. A $^DV/K$ value of 1.00 (± 0.03) was observed.

Oxygen Incorporation into Metabolites. The source of oxygen incorporated into the carbinol metabolites was determined by ESLC−MS analysis of incubations conducted in $^{18}O_2$- and $H_2{}^{18}O$-enriched environments. The fraction of ^{18}O incorporated into the carbinols of furafylline (Figure 3) and cyclohexylline from $H_2{}^{18}O$ after correction for ^{18}O content (47.5%) were calculated to be 81% and 69%, respectively (Table 2). No exchange of $H_2{}^{18}O$ into the carbinols was found in control incubations with authentic carbinols (1 μM) as substrates. The extent of incorporation of water into these carbinols was independently verified by EIGC−MS analysis of the N^7-methyl-O-TMS derivatives of the carbinols generated in the presence of $H_2{}^{18}O$. Oxygen uptake from water was not observed for N^7-methylfurafylline carbinol, N^7-methylcyclohexylline carbinol (Figure 3), or its cyclohexyl ring metabolites. The secondary metabolite of N^7-methylcyclohexylline, 8′-OH-cyclohexylline, incorporated 66% of its oxygen from the medium.

Complementary studies were conducted under an atmosphere of $^{18}O_2$. Substrates were co-incubated pairwise at concentrations which gave adequate amounts of all metabolites (furafylline (5 μM) and N^7-methylcyclohexylline (30 μM) or cyclohexylline (5 μM) and N^7-methylfurafylline (30 μM)). Pairwise incubations were performed to provide verification of $^{18}O_2$ content in the incubations. Similar levels of oxygen incorporation were obtained when the substrates were incubated separately. Reduced concentrations of the inactivating agents were used to ensure adequate formation of metabolites from the N^7-methylxanthines for mass spectrometric analysis. The results of these studies are given in Table 2. Manufacturer-reported content of $^{18}O_2$ as supplied was 95−98%. Figure 3 shows the level of incorporation of ^{18}O from oxygen into the furafylline and *N*-methylcyclohexylline carbinols. Fractional ^{18}O contents in the primary N^7-methylxanthine hydroxylated metabolites (with the exception of the furan metabolites of N^7-methylfurafylline, not shown) were uniformly high and are reported without correction. Fractional ^{18}O content in the 8-methylxanthine carbinols and the secondary metabolite of N^7-methylcyclohexylline, 8′-OH-cyclohexylline, are also given without correction.

These findings show that the majority of the oxygen introduced into the 8′-OH metabolites of furafylline and cyclohexylline originates from water (80% and 70% respectively) with the balance derived from molecular oxygen. Significant exchange of the carbinol oxygen with the medium is precluded by these results. Since almost identical patterns of oxygen incorporation are observed for 8′-OH-cyclohexylline as a primary or a secondary metabolite, we conclude that cyclohexylline rather than N^7-methyl-8′-OH-cyclohexylline is the predominant precursor of this secondary metabolite.

Adduct Studies (Acid Precipitation). Preliminary studies using human liver microsomes revealed significant NADPH-dependent irreversible binding of radiolabeled furafylline and cyclohexylline equivalents to precipitated human liver microsomal protein. Binding was observed using a variety of neutral (methanol, ethanol, acetone) or acidic (trifluoracetic acid, acidic methanol) denaturants. Consistent recovery of total protein (85−89%) was obtained when protein was precipitated by the addition of 0.1 vol of aqueous TFA (1:1 v/v) to microsomal suspensions followed by seven (10 mL) washes of the protein pellets with cold acidic methanol (5% H_2SO_4, v/v) to background. This method was chosen because aliquots of the reaction mixture could be directly analyzed for metabolites by HPLC−RD. Prolonged exposure of protein (1 month, 0 °C) to ^{14}C substrates in trifluoroacetic acid solutions led to minor amounts of covalently bound radioactivity; however, no binding was observed under the conditions employed for these studies. NADPH-dependent protein adduct stability was assessed by further treatment of a selection of the final pellets with acidic methanol at 60 °C for 4 h. Greater than 70% of the covalently bound radioactivity remained bound to the protein (recoveries were not determined) repelleted after this treatment.

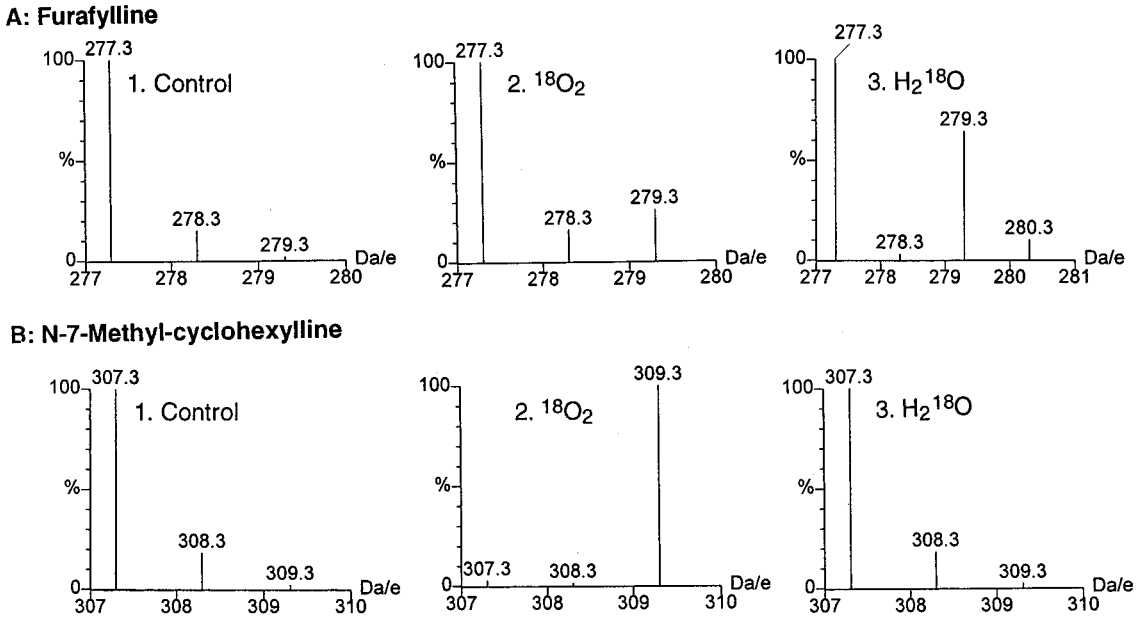

FIGURE 3: ESLC−MS parent ion $[M + H]^+$ isotope clusters of the furafylline (panel A) and N^7-methylcyclohexylline (panel B) carbinols generated by CYP1A2. The spectra shown, after background subtraction, were acquired from (1) control incubations, (2) incubations under an atmosphere of $^{18}O_2$ (substrates co-incubated), and (3) incubations with $H_2{}^{18}O$ (47.5%) in the medium.

Table 2: Incorporation of ^{18}O into Xanthine Metabolites by CYP1A2

metabolite	source of ^{18}O in incubation mixture	
	$H_2{}^{18}O$[a]	$^{18}O_2$[b]
8′-OH-furafylline	81.5 ± 2.3	20.4 ± 1.1
8′-OH-cyclohexylline	68.5 ± 2.9	29.7 ± 1.0
8′-OH-cyclohexylline[c]	65.9 ± 1.5	31.2 ± 2.1
N^7-methyl-8′-OH-furafylline	−0.1 ± 0.1	97.2 ± 2.2
N^7-methyl-8′-OH-cyclohexylline	0.0 ± 0.1	97.9 ± 1.9
N^7-methyl-3′-(cyclohexyl-OH)cyclohexylline (1)[d]	0.0 ± 0.1	98.7 ± 2.3
N^7-methyl-3′-(cyclohexyl-OH)cyclohexylline (2)[d]	0.0 ± 0.1	98.3 ± 1.4

[a] Fraction (given as percent) of ^{18}O observed in metabolites corrected for fraction of $H_2{}^{18}O$ in incubation mixture (47.5%). [b] Fraction of ^{18}O observed in metabolites generated in an $^{18}O_2$ atmosphere with no correction. [c] Secondary metabolite from N^7-methylcyclohexylline. [d] Cyclohexyl ring alcohols.

Table 3: Binding of Xanthine Equivalents to CYP1A2 and Human Liver Microsomal Protein

	substrate			
	furafylline		cyclohexylline	
	CYP1A2	HLM110	CYP1A2	HLM110
microsomal protein (mg)	3	7.7	3.25	9
bound equivalents (pmol mg^{-1})[a]	96 ± 3	76 ± 2	73 ± 3	76 ± 2
CYP1A2 (pmol mg^{-1})	100[b]	80 ± 11[c]	75[b]	80 ± 11[c]
binding ratio	0.96	0.95 ± 0.16	0.97	0.95 ± 0.16

[a] Bound equivalents per milligram of protein in original incubations with expressed CYP1A2 or HL110 microsomes (not corrected for protein loss). [b] Spectral CYP1A2 content in manufacturer's lots as given. [c] Based on indirect spectral estimates (*5*).

The results of radiolabel binding studies conducted with CYP1A2 as well as human liver microsomes are given in Table 3. Similar amounts of binding to HLM110 microsomes were observed for the two methylxanthines after correction for protein content (75−76 pmol/mg of microsomal protein). Higher binding was observed for furafylline (95 pmol mg^{-1}) than for cyclohexylline (75 pmol mg^{-1}) in the case of expressed CYP1A2; however, after normalization for CYP1A2 contents, equivalent binding by both xanthines (0.95 and 0.97 pmol/pmol of CYP1A2, respectively) was found. While the amounts of binding to HLM110 microsomes were similar to our indirect spectral estimate of CYP1A2 content in HLM110 (15 ± 2%), it cannot be assumed that the latter measure is correct (*5*).

The time course of formation of 8′-OH-furafylline and binding of furafylline equivalents to total protein was also determined in human liver microsomes. The P450 concentration was 5.15 μM, and the concentration of furafylline was 30 μM. Furafylline carbinol and irreversibly bound furafylline equivalents reached a plateau by 20 min. The ratio of these two products was maintained at a 5:1 level throughout the time course of the experiment (Figure 4). These results show that bound equivalent and furafylline carbinol formation rates rapidly decline over time in a parallel fashion in accordance with the rapid loss of active enzyme.

Previous studies demonstrated that the rate of loss of CYP1A2 activity caused by furafylline was unaffected by added glutathione (*5*). The current finding that the carbinol oxygen is substantially derived from water suggested that carbinol formation is the result, in part, of the reaction of an electrophilic intermediate with water. This reactive species could conceivably be the proximate inactivating intermediate and might react with microsomal proteins as well. Glutathione, *N*-acetylcysteine, and cyanide salts have been successfully employed to trap electrophilic intermediates such as imines, quinones, and iminoquinones released from P450 enzymes. The effect of these agents on binding and carbinol formation was investigated in CYP1A2 lymphoblastoid cell microsomes (Table 4). A slight decrease in the amount of carbinol formed was observed for furafylline (4%) and cyclohexylline (7%) in the presence of glutathione; however, no new radioactive peaks were observed in the radiochromatograms. In the case of cyclohexylline, a single new

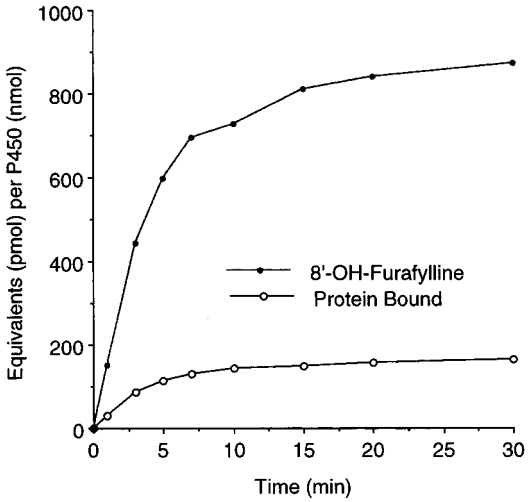

FIGURE 4: Time-dependent accumulation of 8′-OH-furafylline and protein-bound equivalents generated by incubation of HLM110 microsomes with [8-^{14}C]furafylline (30 μM) in the presence of NADPH. Aliquots of the reaction mixtures were removed at the times shown post addition of NADPH, quenched by addition to aqueous TFA, and assayed for products. Amounts of products are expressed per nanomole of total microsomal P450.

Table 4: Effect of Trapping Agents on CYP1A2-Catalyzed Carbinol Formation and Protein Binding[a]

	substrate			
	furafylline		cyclohexylline	
trapping agent	8′-carbinol	adduct	8′-carbinol	adduct
control	1.25	0.23	1.84	0.23
NaCN (1 mM)	1.25	0.23	1.84	0.24
N-acetylcysteine (8 mM)	1.25	0.24	1.85	0.24
glutathione (2 mM)	1.20	0.24	1.71[b]	0.23

[a] CYP1A2 microsomes (Gentest) and furafylline or cyclohexylline (30 μM) were incubated with NADPH for 30 min in the presence of the indicated tapping agents. Values given are xanthine equivalents (nmol) either as 8′-carbinol or bound to microsomal protein (adduct) in the original incubation mixtures. Protein was precipitated with TFA, washed to background with acidic methanol (5%, v/v, H_2SO_4), and counted. The supernatants were analyzed for carbinols by LC−RD. Standard deviations were less than 3% of the values shown ($n = 3$). [b] Significantly different from control ($p < 0.05$).

glutathione-adducted metabolite would have likely been observed due to the higher specific activity of this substrate. Inclusion of NaCN, glutathione, or *N*-acetylcysteine in the incubation mixture had no effect on the extent of binding to microsomal protein. These results demonstrate that few, if any, electrophilic intermediates which might be generated by CYP1A2 catalysis are trapped by these agents.

Adduct Studies (SDS−PAGE). CYP1A2 lymphoblastoid cell microsomes were incubated with the [^{14}C]xanthines in the presence and absence of NADPH as before. Aliquots of the reaction mixtures were fractionated by SDS−PAGE, and the distribution of radioactivity (Figure 5) was assessed by scintillation counting of the gel slices. The grid of gel slices was arranged such that the region between CYP2C9 and CYP2C19 (loaded into adjacent lanes) was taken in a single 4-mm slice. NADPH-dependent binding was localized to those slices taken between the bracketing markers. Most, if not all, of the protein-bound radioactivity migrated in a single band on the gels. Aliquots of the original reaction mixtures were also analyzed for carbinol and protein-bound equivalents. The results of these studies are summarized

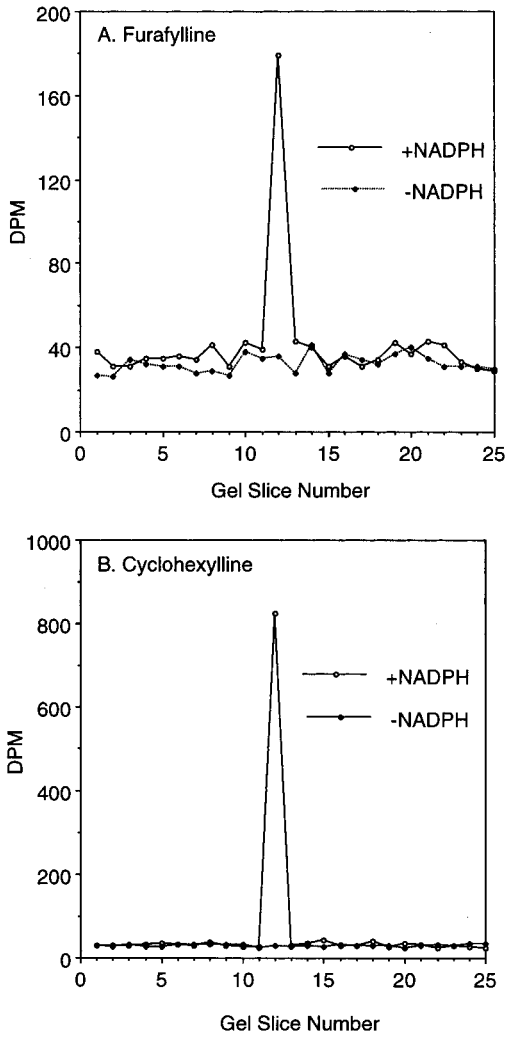

FIGURE 5: Radiolabeled furafylline (11 dpm pmol^{-1}) or cyclohexylline (61 dpm pmol^{-1}) was incubated with microsomes isolated from lymphoblastoid cells expressing CYP1A2 (330 ± 15 pmol) in the presence or absence of NADPH. The distribution of radioactivity (given in dpm without background subtraction) after SDS−PAGE resolution of microsomal proteins was determined by scintillation counting of gel slices (4 mm) dissolved in hyamine hydroxide. Purified CYP2C19 (slice 11) and CYP2C9 (slice 13) loaded in adjacent lanes were used to localize slice 12 in each lane, which contained most of the radioactivity on the gel. Aliquots of the reaction mixtures loaded onto the gels represented 3.8% of the original sample.

in Table 5. Partition ratios calculated as total carbinol divided by adduct were 5.0 and 7.6 for furafylline and cyclohexylline, respectively. As before, acid-precipitated bound radioactive equivalents were roughly 95% of CYP1A2 content estimates. After correction for loss of protein, the amounts of bound radioactivity by the two methods were not significantly different. These results show that total protein binding is localized to protein which migrates in a single 4-mm band,[2] and they are consistent with selective binding to CYP1A2.

[2] Markers CYP2C9 and CYP2C19 were selected on the basis of electrophoretic mobility relative to the adduct. Purified CYP1A2 was not available to us at that time. We have recently found that purified, reconstituted human CYP1A2 expressed in bacculovirus produces cyclohexylline carbinol with the same fraction of oxygen derived from water and an adduct of similar apparent MW by SDS−PAGE (unpublished observations from this laboratory).

Table 5: Partition Ratios for Inactivation of CYP1A2 by Furafylline and Cyclohexylline

xanthine equivalents as[a]	furafylline	cyclohexylline
8′-OH-carbinol (total)	1750 ± 50	2647 ± 140
8′-OH-carbinol (from H_2O)[b]	1426 ± 74	1813 ± 170
CYP1A2 adduct (SDS−PAGE)	346 ± 18[e]	349 ± 6[e]
partition ratio[c]	5.05 ± 0.41	7.58 ± 0.72
protein bound (acid precipitation)	311 ± 6	312 ± 5
corrected protein bound[d]	370 ± 11[e]	345 ± 14[e]

[a] Amounts of carbinol and bound equivalents (pmol per incubation) formed upon incubation of the xanthines (30 μM) with CYP1A2 (330 ± 13 pmol, spectral 450 content) for a period of 30 min. [b] Total carbinol times fraction of oxygen derived from water (Table 2). [c] Total carbinol divided by the amount of adduct based on SDS−PAGE results. [d] Corrected value based on fraction of original protein recovered in the final acid-washed pellet. [e] Not significantly different ($p > 0.05$).

Significant NADPH-dependent binding of N^7-methylfurafylline to microsomes derived from human liver or lymphoblastoid cells expressing CYP1A2 was not detected; however, binding of N^7-methylcyclohexylline equivalents was observed. This is consistent with the results of the inactivation studies if binding to protein is a marker for inactivation. The fact that large amounts of cyclohexylline and its further metabolite, 8′-OH-cyclohexylline, are observed in incubations of N^7-methylcyclohexylline with CYP1A2 but the corresponding metabolites of N^7-methylfurafylline (particularly 8′-OH-furafylline) are not suggested that the inactivation observed might be due to further metabolism of cyclohexylline rather than to oxidation of the substrate itself. To address this issue, incubations of CYP1A2 with radiolabeled N^7-methylcyclohexylline (100 μM) were analyzed for bound equivalents (SDS−PAGE) and metabolites. A 30-min incubation with 208 pmol of CYP1A2 produced 703 ± 42 pmol of 8′-OH-cyclohexylline and 85 ± 4 pmol of CYP1A2 adduct. Radioactivity on the gel was localized as before to a single gel slice. The demethylated carbinol-to-adduct partition ratio from this experiment (8.3 ± 0.9) was not significantly different ($p > 0.1$) from that of cyclohexylline itself (7.6 ± 0.7). These results show that the observed inactivation can be accounted for by conversion of the primary metabolite cyclohexylline to its 8′-carbinol rather than by oxidation of N^7-methylcyclohexylline itself.

DISCUSSION

An essential feature of mechanism-based inhibition is the catalysis-driven covalent attachment of the suicide substrate to elements of the enzyme active site (*16*). Our studies demonstrate that oxidation of furafylline and cyclohexylline by cDNA-expressed human CYP1A2 results in a stable, one-to-one adduct of xanthine with CYP1A2 protein. Xanthine binding to other proteins in the lymphoblastoid cell microsomes was not detected after SDS−PAGE resolution of microsomal proteins. These results provide a molecular basis for the time-dependent loss of CYP1A2 activity caused by furafylline, confirm our earlier conclusion that the furan moiety is not directly involved in the inactivation process, and demonstrate that the protein adduct is reasonably stable.

The only metabolites of these xanthines produced by CYP1A2 are the corresponding 8′-carbinols, suggesting that carbinol formation and binding to the enzyme might evolve from a common intermediate. The fact that the intermolecular deuterium isotope effect for 8′-hydroxylation of furafylline ($^DV/K = 1.8 \pm 0.1$) determined here is similar to the noncompetitive isotope effect on the loss of CYP1A2 activity in human liver microsomes ($^Dk_{inact}/^DK_I = 2.4 \pm 0.8$) supports this proposal with the caveat that K_m and K_I may not always be equivalent (*16*). Further, the low partition ratios for furafylline (5) and cyclohexylline (7.5) indicate that the reactive intermediate has a high probability of finding a target in the enzyme active site.

Scheme 1

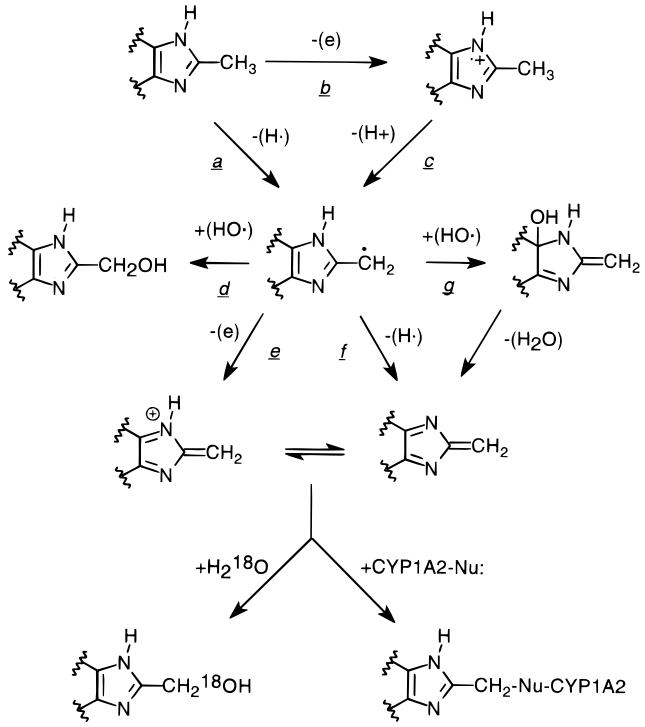

The majority of the oxygen introduced into the 8′-methyl carbinol metabolites of furafylline (80%) and cyclohexylline (70%) by CYP1A2 is derived from water, with the balance originating from molecular oxygen. Formation of electrophilic species such as the exocyclic 8-methyleneimidazolenine (imidazomethide) or its conjugate acid (Scheme 1) are indicated by these findings. A similar dehydrogenated intermediate (3-methylene indolenamine) has been proposed to account for the extensive reaction of the P450-activated exocyclic carbon of 3-methylindole with protein thiols, nucleophilic trapping agents, and the medium. Significantly, a minimum of 85% of the indole-3-carbinol is derived from addition of water, and high intramolecular isotope effects ($k_H/k_D = 5$) and low $^DV/K$ isotope effects are noted for formation of carbinol and *N*-acetylcysteine conjugates (*17*, *18*). These mechanistic parallels support the hypothesis that a major fraction of the inactivating xanthines processed by CYP1A2 evade normal oxygen rebound in favor of an alternate pathway which renders the 8′-carbon susceptible to reaction with the medium or nucleophilic active site amino acids.

The presence of glutathione or cysteine substantially reduces binding of 3-methylindole metabolites to protein (*18*, *19*). The amounts of enzyme conjugate and carbinol found following incubation of cyclohexylline or furafylline with CYP1A2 were unchanged in the presence of cyanide or *N*-acetylcysteine. Glutathione marginally reduced the amount

of carbinol from furafylline (4%) and cyclohexylline (7%); however, no new radioactive compounds were found upon analysis of the supernatants. These results, and the lack of labeling of other microsomal proteins, lead to the conclusion that either the putative imidazomethide does not react rapidly with these nucleophiles or the local concentrations of the trapping agents are insufficient to successfully compete with water addition. One intriguing hypothesis, currently under investigation, is that water addition is accomplished within the confines of the CYP1A2 active site.

One corollary to our mechanistic proposal is that substrate processing by conventional oxygen rebound chemistry is not detrimental to enzyme function. Substantial amounts of the 8′-carbinols of N^7-methylfurafylline and N^7-methylcyclohexylline (2.7 and 11.2 nmol/nmol of CYP1A2) are formed in 30-min incubations with CYP1A2. Since molecular oxygen is the only source of oxygen in these metabolites, catalytic function should be preserved. The results with N^7-methylfurafylline fully support this supposition. By contrast, time-dependent loss of liver microsomal CYP1A2 activity as well as covalent attachment of N^7-methylcyclohexylline equivalents to recombinant CYP1A2 protein is observed. These discrepant findings were reconciled by partition ratio analysis and ^{18}O studies which demonstrated that the degree of binding to CYP1A2 protein can be fully accounted by further processing of the primary metabolite cyclohexylline to 8′-OH-cyclohexylline. The N^7-methylxanthine data are therefore entirely consistent with the hypothesis that oxygen rebound preserves enzyme function and that enzyme inactivation and water incorporation into the carbinol are products of the two electron oxidized reactive intermediates of furafylline and cyclohexylline.

The high intramolecular isotope effects for carbinol formation from the four monodeuterated 8-methylxanthines argue for a linear, symmetrical transition state (*20*) for hydrogen removal. While the possibility that two distinct modes of C−H bond cleavage would produce high and similar intramolecular isotope effects cannot be rejected out of hand, it is reasonable to assume that each of these substrates, regardless of the source of carbinol oxygen, is subject to a common mechanism of hydrogen removal. By this reasoning, reaction trajectories marked by the formation of xanthine *N*-oxides or hydroxylamines, which might rearrange to the carbinols (*21*) with incorporation of water from the medium, do not appear to be involved in the metabolism of these substrates. Likewise, initial hydrogen atom abstraction from the imidazole nitrogen does not appear to be a viable option. Since oxygen rebound is observed, we conclude that a heteroaromatic methyl radical is a common intermediate for all four substrates.

High isotope effects are often observed for those P450-catalyzed oxidation reactions which are widely held to be triggered by homolytic cleavage of carbon−hydrogen bonds such as aliphatic hydroxylation, O-dealkylation, benzylic and allylic hydroxylation, N-dealkylation of amides, and dehydrogenation of alkanes (*22*). The high isotope effects observed for the 8-methylxanthines are consistent with, but not proof of, a hydrogen atom transfer (HAT) mechanism (Scheme 1, path a). An alternative route to the heteroaromatic methyl radical (Scheme 1, path b−c) initiated by electron abstraction from the imidazole ring cannot be ruled out since single electron transfer (SET) pathways have been envisioned to underlie P450-catalyzed reactions such as the oxidation of dihydropyridines (*22*) and, more controversially, dealkylation of aryl alkylamines (*23*−*26*). However, when P450 is the oxidant under normal turnover conditions, these reactions proceed with low inter- and intramolecular isotope effects for carbon−hydrogen bond cleavage. While a SET pathway cannot be rigorously excluded at this time, we note that both alternatives converge on the heteroaromatic radical intermediate and that it appears likely, on the basis of the isotope effect data, that only one of these two alternatives is common to all of the xanthines studied here.

Four pathways for reaction of the iron-bound hydroxyl radical with the heteroaromatic radical are considered here (Scheme 1). One or more post-abstraction pathways must compete with the reaction sequence widely held to dominate P450 hydroxylation chemistry (path d). While proximate recapture rates can be very fast (*22*, *27*), it is clear that alternative post-abstraction processes leading to dehydrogenation (path e or f), allylic hydroxylation (path g), and oxygen rebound at epimeric sites (*28*, *29*) may operate during substrate oxidation.

Single electron removal (path e) would produce electrophilic cationic intermediates certainly capable of reacting with protein or water. Cationic intermediates form the basis of one of two proposed pathways for P450-catalyzed dehydrogenation reactions (*22*, *30*). More generally, the existence of requisite cationic intermediates as an alternative to radical processes in P450 hydroxylation reactions has been discounted; however, cationic character, perhaps as part of a transition state ensemble, may have been detected (*27*). The observation of exclusive oxygen rebound chemistry in the formation of the N^7-methylxanthine carbinols is not consistent with this alternative unless the N^7-methyl substituent selectively promotes reaction of a cationic intermediate with hydroxide anion ligated to heme. One might speculate that loss of the imidazole proton may serve to "trap" incipient transition-state cationic character; however, no precedent exists for this proposal.

Removal of the second electron in the form of a hydrogen atom (path f) is an appealing option since delocalization of radical density into the imidazole ring may promote homolysis of the imidazole N−H bond by the proximate iron-bound hydroxyl radical. Dehydrogenation via sequential hydrogen atom abstraction from adjacent carbon atoms has been proposed by a number of laboratories, and the partition between desaturation and recapture may be enhanced when the initially formed radical is stabilized by an adjacent pi bond (*31*−*35*). A similar effect might explain the preponderance of dehydrogenation apparently observed with the xanthines. Further, since hydrogen atom abstraction from nitrogen is not available for N^7-methyl derivatives of furafylline and cyclohexylline, oxygen rebound chemistry would be expected as the only alternative, a result which we observe.

Allylic recapture of the heteroaromatic radical (path g) followed by loss of water has been proposed as an alternative to direct dehydrogenation in the oxidation of 3-methylindole (*18*). Along these lines, bioactivation of phenacetin by P450 very likely involves distal recapture at an aromatic carbon via hydrogen atom abstraction from nitrogen and recapture of the aromatic iminium radical at the para position in addition to formation of the hydroxylamine by recombination

(*36*, *37*). Activation of the 8-methylxanthines via this pathway is consistent with our findings since the oxygen transferred from the heme iron to a member of the imidazole ring (shown as C-5 in Scheme 1) would be lost by aromatization to the imidazomethide. However, one again might expect to observe some evidence for the anticipated products of allylic recapture in the case of the N^7-methylxanthines.

Our results show that oxidative attack at the 8-methyl group of furafylline and cyclohexylline results in the preferential formation of a two electron oxidized intermediate by an unusual mechanism that permits efficient reaction with CYP1A2 active site protein residues or the medium. The 8′ carbon is the most likely site for attack by active site amino acids; however, attack directed at other positions is also possible, although these species would not be expected to be particularly stable. More limited studies in human liver microsomes reported here provide results in general agreement with our conclusions relative to our findings with expressed CYP1A2. However, product profile comparisons indicate that other enzymes in human liver microsomes also process these substrates. Therefore, it would be premature to conclude that the covalent binding of the xanthines to human liver microsomal protein is confined to CYP1A2.

Selective covalent binding to a single nucleophilic amino acid residue proximate to the heme iron may occur, particularly if the binding interactions which direct the metabolism of the inactivating xanthines toward the 8′ carbon persist along the reaction trajectory to adduct. Homology models for the CYP1A family have been constructed recently for the purpose of defining active site elements which might be important in substrate binding (*38*, *39*). Furafylline has been proposed to dock with human CYP1A2, with interaction of the furan with Phe125 directing the 8-methyl (flanked by Thr124 hydrogen bonded to the N^9-imidazole nitrogen) toward the heme iron (*38*). Solution NMR studies indicate that the tautomeric xanthine imidazole proton of 1,3-dimethylxanthine resides predominantly, if not exclusively, at the N^7 nitrogen (*40*) in agreement with the model. However, the tautomeric distribution for the xanthines studied here in solution and the effects of the active site environment on that distribution are unknown. In the case of the N^7-methylxanthines, where a hydrogen bond to the N^9 position might still be expected, most of the metabolic activity is redirected to the N^3 substituents. This loss of specificity engendered by the presence of a 7-methyl group suggests that a hydrogen bond to the xanthine N^9-imidazole nitrogen may not be a primary determinant of substrate orientation. Conversely, it appears that a dominant binding interaction is removed upon 7-methylation. Further study of the 8-methylxanthine adducts and the pattern of metabolic products produced from other xanthine analogues may provide further information to complement efforts to define CYP1A2 tertiary structure.

REFERENCES

1. Ortiz de Montellano, P. R., and Correia, M. A. (1995) In *Cytochrome P450: Structure, Mechanism and Biochemistry* (Ortiz de Montellano, P. R., Ed.) pp 305−366, Plenum Press, New York.
2. Von Wachenfeldt, C., and Johnson, E. F. (1995) In *Cytochrome P450: Structure, Mechanism and Biochemistry* (Ortiz de Montellano, P. R., Ed.) pp 183−223, Plenum Press, New York.
3. Eaton, D. L., Gallagher, E. P., Bammler, T. K., and Kunze, K. L. (1995) *Pharmacogenetics 5*, 249−274.
4. Sesardic, D., Boobis, A., Murray, B., Murray, S., Segura, J., De La Torre, R., and Davies, D. (1990) *Br. J. Clin. Pharmacol. 28*, 651−663.
5. Kunze, K. L., and Trager, W. F. (1993) *Chem. Res. Toxicol. 6*, 649−656.
6. Kunze, K. L., Weinkers, L. C., Thummel, K. E., and Trager, W. F. (1996) *Drug Metab. Dispos. 24*, 414−421.
7. Tassaneeyakul, W., Birkett, D. J., Veronese, M. E., MacManus, M. E., Tukey, R. H., Quattrochi, L. C., Gelboin, H. V., and Miners, J. O. (1993) *J. Pharmacol. Exp. Ther. 265*, 401−407.
8. Tassaneeyakul, W., Birkett, D. J., Veronese, M. E., MacManus, M. E., Tukey, R. H., and Miners, J. O. (1994) *Pharmacogenetics 4*, 281−284.
9. Gallagher, E. P., Kunze, K. L. Stapleton, P. L., and Eaton, D. L. (1996) *Toxicol. Appl. Pharmacol. 141*, 595−606.
10. Tarrus, E., Cami, J., Roberts, D. J., Spickett, R. G. W., Celdran, E., and Segura, J. (1987) *Br. J. Clin. Pharmacol. 23*, 9−18.
11. Boobis, A. R., Lynch, A. M., Murray, S., de la Torre, R., Solans, A., Farre, M., Segura, J., Gooderham, N. J., and Davies, D. S. (1994) *Cancer Res. 54*, 89−94.
12. Lister, J. H. (1996) *Heterocyclic Compounds, The Purines*, Vol. 54, Suppl. 1, Chapter IV, John Wiley and Sons, New York.
13. Ling, K. J., and Hanzlik, R. P. (1989) *Biochem. Biophys. Res. Commun. 160*, 844−849.
14. Hanzlik, R. P., Hogberg, K., Moon, J. B., and Judson, C. M. (1985) *J. Am. Chem. Soc. 107*, 7164−7167.
15. Gillette, J. R., Darbyshire, J. F., and Sugiyama, K. (1994) *Biochemistry 33*, 2927−2937.
16. Silverman, R. (1988) *Mechanism-Based Enzyme Inactivation: Chemistry and Enzymology*, Vol. 1, CRC Press, Boca Raton, FL.
17. Thorton-Manning, J., Appleton, M. L., Gonzalez, F. J., and Yost, G. S. (1996) *J. Pharmacol. Exp. Ther. 276*, 21−29.
18. Skiles, G. L., and Yost, G. S. (1996) *Chem. Res. Toxicol. 9*, 291−297.
19. Nocerini, M. R., Carlson, J. R., and Yost, G. S. (1985) *Toxicol. Appl. Pharmacol. 81*, 75−84.
20. More O'Ferral, R. A. (1970) *J. Chem. Soc. B*, 785−790.
21. Zvilichovsky, G. (1977) *Tetrahedron 33*, 2259−2266.
22. Ortiz de Montellano, P. R. (1995) In *Cytochrome P450: Structure, Mechanism and Biochemistry* (Ortiz de Montellano, P. R., Ed.) pp 245−303, Plenum Press, New York.
23. Guengerich, F. P., Ozakaki, O., Seto, Y., and MacDonald, T. L (1995) *Xenobiotica 25*, 689−709.
24. Guengerich, F. P., Yun, C., and MacDonald, T. L. (1996) *J. Biol. Chem. 271*, 27321−27329.
25. Karki, S. B., and Dinnocenzo, J. P. (1995) *Xenobiotica 25*, 710−724.
26. Karki, S. B., Dinnocenzo, J. P., Jones, J. P., and Korzekwa, K. R. (1995) *J. Am. Chem. Soc. 117*, 3657−3664.
27. Newcomb, M., Tadic-Biadatti, M. L., Chestney, D. L., Roberts, E. S., and Hollenberg, P. F. (1995) *J. Am. Chem. Soc. 117*, 12085−12091.
28. Groves, J. T., and Han, Y. (1995) In *Cytochrome P450: Structure, Mechanism and Biochemistry* (Ortiz de Montellano, P. R., Ed.) pp 3−48, Plenum Press, New York.
29. White, R. E., Miller, J. P., Favreau, L. V., and Bhattacharyya, A. (1988) *J. Am. Chem. Soc. 108*, 6024−6031.
30. Ortiz de Montellano, P. R. (1989) *Trends Pharmacol. Sci. 10*, 354−359.
31. Rettie, A. R., Boberg, M., Rettenmeier, A. W., and Baillie, T. A. (1988) *J. Biol. Chem. 263*, 13733−13738.
32. Korzekwa, K. R., Trager, W. F., Nagata, K., Parkinson, A., and Gillette, J. R. (1990) *Drug Metab. Dispos. 18*, 974−979.
33. Kassahun, K., and Ballie, T. A.(1993) *Drug Metab. Dispos. 21*, 242−248.

34. Watanabe, Y., and Ishimura, Y. (1989) *J. Am. Chem. Soc. 111*, 410−411.
35. Vyas, K. P., Kari, P. H., Prakash, S. R., and Duggan, D. E. (1990) *Drug Metab. Dispos. 18*, 218−222.
36. Koymans, L., Van Lenthe, J. H., Donne-Op Den Kelder, M., and Vermeulen, N. P. E. (1990) *Mol. Pharmacol. 37*, 452−460.
37. Hinson, J. A., Nelson, S. D., and Gillette, J. R. (1979) *Mol. Pharmacol. 15*, 419−427.
38. Lewis, D. F. V., and Lake, B. G. (1996) *Xenobiotica 26*, 723−753.
39. Lozano, J. J., Lopez-de-Brinas, E., Centeno, N. B., Guigo, R., and Sanz, F. L. (1997) *J. Comput. Aided Mol. Des. 11*, 395−408.
40. Lichetenberg, D., Bergmann, F., and Neiman, Z. (1971) *J. Chem. Soc. C*, 1676−1682.

BI973011M